Advances in Science and Technology Research Journal

Advances in Science and Technology Research Journal 2024, 18(4), 410–419
https://doi.org/10.12913/22998624/189848
ISSN 2299-8624, License CC-BY 4.0

Received: 2024.03.21
Accepted: 2024.06.11
Published: 2024.06.20

Carbide Cutting Tool Coatings Characterization of 8YSZ

Shaimaa J. Kareem[1], Wurood Asaad M.[2*], Sundus Abbas[1], Haydar Al-Ethari[3]

[1] Department of Ceramic and Building Materials Engineering, College of Materials Engineering, Babylon University, Iraq

[2] Al Salam College University, Iraq

[3] College of Materials Engineering, University of Babylon, Iraq

* Corresponding author's e-mail: wurood.a.midab@alsalam.edu.iq

ABSTRACT

Using a duplex deposition of TiO_2/8YSZ on a carbide cutting tool, a successful sol-gel procedure was achieved, resulting in high homogeneity, good dispersion, and a low average value of surface roughness (223.6 nm). Thermal experiments were done to see how well the coating layers could withstand heat transfer and thermal deterioration. Residual stresses for coated and uncoated carbide cutting tools are measured after thermal shock (thermal shock). Both were immediately chilled in ice water after being heated for 90 minutes for coated inserts and 30 minutes for uncoated inserts at 500, 600, 700, 800, 900, and 1200 °C. For inserts, thermal shock from 900 °C results in significantly different damage mechanisms. The uncoated outside surface is still delineated by a crack network and is surrounded by nearby homogenous cells, but the coated insert (sol-gel TBC) in this case really has a few tiny cracks beginning at the edge. The coated insert fails after being heated to 1200 °C and then cooled in water to freezing which is caused the start of the duplex coating degradation.

Keywords: coated carbide cutting tool, sol gel, thermal shock, TiO_2/8YSZ.

INTRODUCTION

Carbide tools are extensively employed in several industries such as metalworking, machining, and manufacturing due to their high hardness, wear resistance, and toughness. Nonetheless, carbide-cutting tools are prone to surface wearing, mechanical deformation "chipping", and thermal strain during the cutting process. These parameters affect the performance and lifespan [1]. People have put tremendous efforts to resolve such crucial issues. One way to address such issues is making coating layers to protect the surface of the carbide cutting. These layers are usually thin withing a range of nanometers.. The coating layer changes the surface mechanical characteristics and enhance its durability The coated carbide tool becomes tougher, less prone to chip or crack, improving thermal stability. Scientists have used high-temperature resistant nanomaterials, high hardness, and reducing friction between the tool and the workpiece. This surface arming makes the carbide withstand the high temperatures that is generated during the cutting process [2]. In some cases where high heat evolves, layers of coating materials with high thermal stability and low thermal conductivity are employed to create thermal barrier coatings. Three fundamental parts govern the successful coating system. TBCs: a metal substrate, a metallic bonding coating (BC), and a ceramic top coating (TC). Deep understanding of TBC composition, mechanical characteristics, and failure mechanisms are essential to improve them [3–6]. Because of its unique properties, yttria-stabilized zirconia (YSZ) is a type of ceramic material that is widely used. Due to great mechanical strength, hardness, and temperature stability, it effectively resists deterioration.

The high chemical resistance makes it powerful in harsh chemical environments. Overall, the

unique combination of properties of YSZ makes it a highly versatile and useful material for a wide range of applications [7, 8]. One method of nanomaterial deposition is the *sol-gel* method which potentially utilized for improved TBCs. This is because of the crystal size affects the top coating decreased the thermal conductivity. Sol-gel processes are commonly used in the production of various materials, including ceramics, glasses, and composites. Sol-gel processes are used in a wide range of applications, including coatings, catalysts, sensors, electronic materials, and biomaterials, among others [9, 10].

The properties of the resulting materials can be managed by controlling the composition of the precursor sol, the reaction conditions, the drying and annealing processes where gels transform to a solid material. Sol-gel offer several advantages over other methods of materials synthesis, including the ability to produce highly homogeneous and pure materials, the potential for precise control over the composition and structure of the materials, and the ability to create complex shapes and structures.

Wang et al. [11] have achieved the laser micro-hole drilling quality on nickel base alloys coated with thermal barriers and having a 300 μm thick ceramic layer (yttria-stabilized zirconia) by flame spraying and a 100 μm thick NiCrAlYTa bond coat (BC). Vignesh et al. [12] have investigated using thermal barrier coatings made of YSZ top coat and NiCoCrAlY. The bond coat and top coat were applied using an atmospheric plasma spray coating device (spraying gun). The foundation material is a nickel-based super alloy. To find out how long TBCs will last, one of the most popular accelerated tests was applied to the coated samples: thermal cycling. This study examines the geometric variables, thermal physical properties, coating-chip contact characteristics, and coating-substrate diffusion layer factors that affect cutting temperature when using coated tools. These influencing factors' decision-making procedures are reported by Zhao et al. [13] The purity and crystallographic structure of the final nanocrystalline ceria-yttria co-stabilized zirconia (CYSZ) powder product were examined in relation to the thermal shock process using X-ray diffraction.

The presented study aims at adjusting machining qualities under high conditions by improving thermal barrier properties for carbide cutting tools and reducing surface roughness through nano particles deposition on it by sol-gel technique.

EXPERIMENTAL WORK

Substrate

Tungsten cemented carbide inserts of type (K01) were used in this investigation. All the inserts have the same geometry and are designated as [TNMG 160408] [14] by the American National Standard Institute (AISI). The used carbide inserts have a square cross shape measuring 13×13×5 mm. Their composition is 3.6% Co, 77% W, 7.7% C, 5% Ti, 6.7% O in weight percentage. Before the thermal shock for uncoated carbide insert, XRD analysis was used to identify the products for the substrate (carbide insert). For the WC and Co peaks were displayed in Figure 1 and Figure 2.

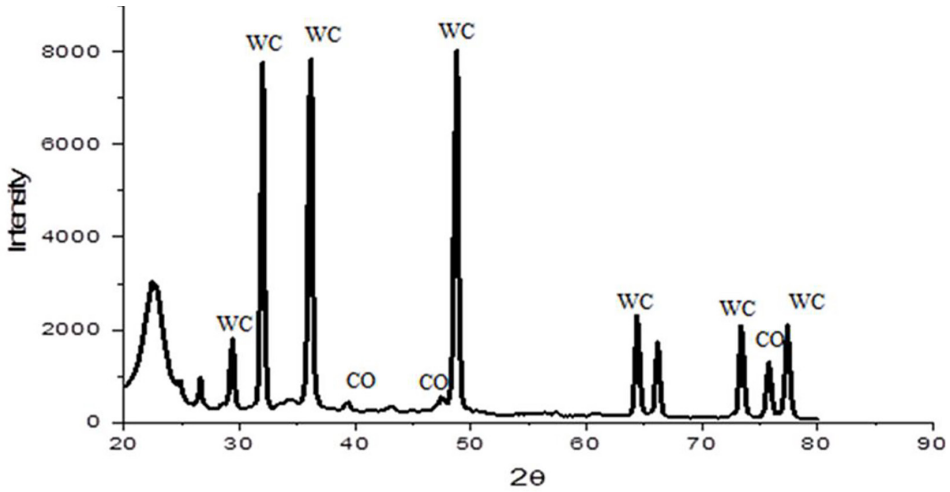

Figure 1. XRD pattern of carbide cutting tool

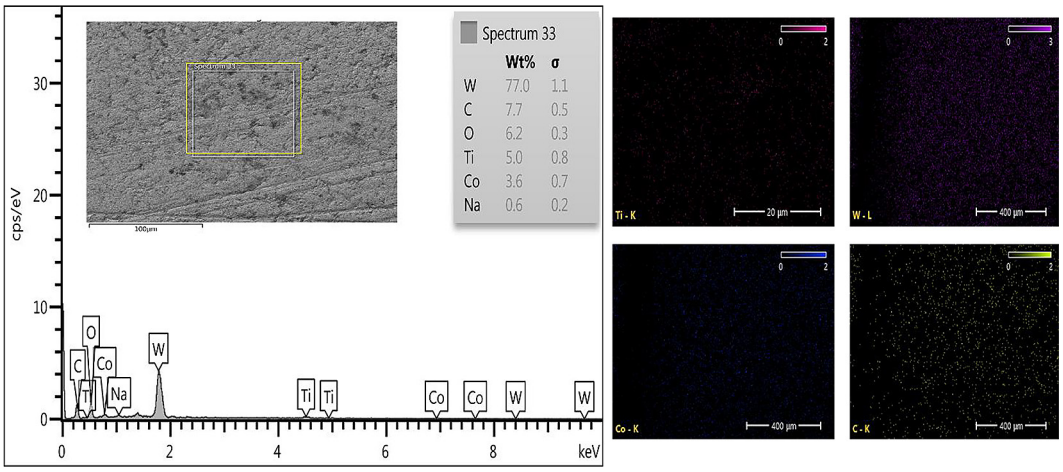

Figure 2. EDS mapping of carbide cutting tool surface

Coating deposition

Titania coatings can be prepared by the sol-gel method. The general steps for preparing a Titania sol-gel coating are [15]: the precursor chemicals titanium tetraisopropoxide, TTIP) are dissolved in a solvent, usually an alcohol like ethanol, to form a clear solution called sols. The sols are then applied onto the substrate using dip-coating process. The coated substrate is then left to dry in furnace at 330 °C to remove the solvent. The final properties of the titania coating can be tuned by adjusting the precursor concentration, solvent type, coating thickness, and heat-treatment conditions.

Yttria-stabilized zirconia (YSZ) coatings can be prepared by the sol-gel method. The process includes preparing the sol-gel coating solution by hydrolyzing and condensing the zirconium alkoxide ($Zr(OC_3H_7)_4$) and yttrium alkoxide (yttrium II tris isopropoxide) using ethanol as a solvent. The YSZ sol-gel coating solution is applied to the substrate coated with titania layer using dipping method. The coated substrate is dried in furnace at 330 °C to remove the solvent and water formed during the hydrolysis reaction; the dried substrate is heated in a furnace at 700 °C for two hours to remove any remaining organic materials and to density the YSZ coating.

Characterization of the coating layer

The surface roughness of coated and uncoated surfaces was examined with atomic force microscopy (AFM), while FE-SEM was used for imaging and analyzing the surface structure at high magnification. To perform the tests, the samples were prepared by cleaning and mounting it on a suitable substrate.

Thermal tests for coating layers

Two thermal tests were conducted to determine the ability of the coating layers to resist the transfer of the heat and the thermal degradation. These tests are the thermal conductivity test and the test for thermal shock resistance by water quenching.

Thermal shock resistance test

The coating layers were undergone for thermal shock tests. After 90 minutes of heating at 1200, 1000, 900, 800, 700, 600, and 500 °C for the coated inserts and 30 minutes of heating at the same temperatures for the uncoated inserts, the inserts were cooled in freezing water for 5 seconds. To document the coating spallation, the surface of the cooled samples was photographed. The cracks in the ceramic coating for coated inserts compared to that for uncoated inserts were studied to determine the coating's thermal shock resistance. SEM was employed for microstructure study for better understanding the failure mechanisms of TBCs under thermal shock conditions. A high temperature and a quick cooling rate are prerequisites for thermal shock [16–18, 26].

RESULT AND DISCUSSION

FESEM and AFM tests

Figure 3b shows the SEM picture of a duplex coating (TiO_2/8YSZ) on the carbide tool, along with the coated insert, as seen in Figure 3a.

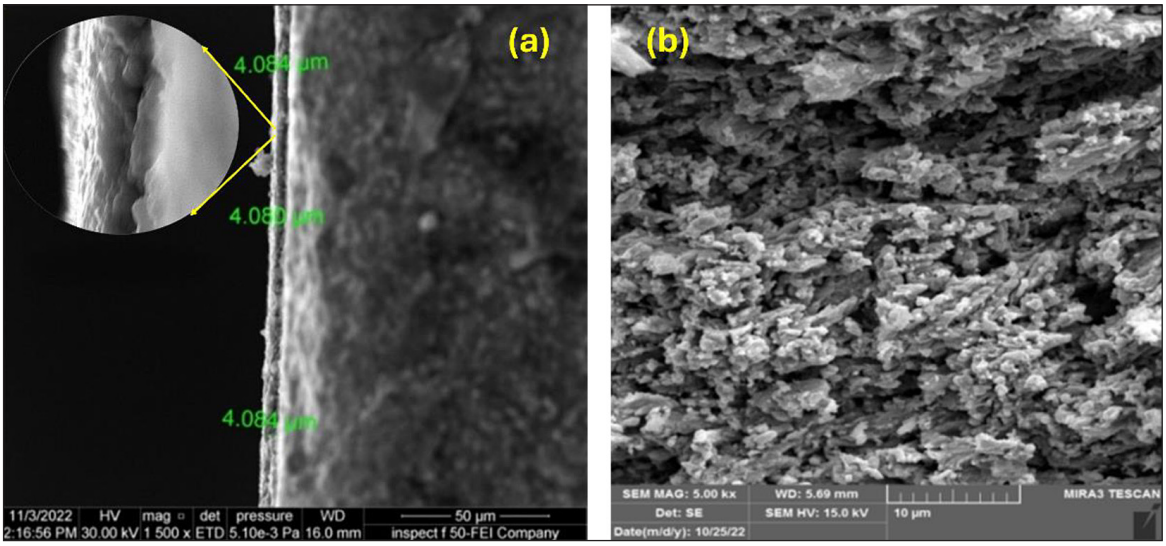

Figure 3. FESEM image of coating TiO_2/8YSZ on carbide insert by sol gel, (a) cross section; (b) coating surface

The EDS spectra of the coated 8YSZ sections of the tool are displayed in detail; as can be seen in Figure 4, the presence of Y, Zr, O, and Ti in the coating region confirms the deposition of TiO_2/8YSZ layer.

The AFM maps of the structured surfaces for coated and uncoated cutting inserts are shown in Figures 5a, 5b, 5c. A duplex layer of TiO_2/8YSZ exhibits strong homogeneity, good distribution, and had a minimum average value of surface roughness 223.6 nm as the titania led to achieve a good adhesive strength [19]. The monolayer of 8YSZ has a surface roughness of 468.7 nm with a lesser homogeneity as clear from Figure 5. The uncoated insert, however, has a surface roughness rating of 903.1 nm. Using the image analysis software, the average and size distribution of the particles were calculated by counting more than 475 particles from the AFM image. The average particle size equals 80.37 nm with high homogeneity distribution for duplex coating. 8YSZ TBC with smallest particle size shows better thermal shock resistance due to low elastic modulus and residual stress [23].

Thermal tests

Figure 6 shows several images taken of coated and uncoated inserts after being heated to 500, 600, 700, 800, 900, 1000, and 1200 °C for 90 minutes for coated inserts and 30 minutes for uncoated inserts. Both coated and uncoated were quenched in frozen water.

After direct quenching from 600 °C and below, both samples remain essentially undamaged.

Table 1. Thermal shock effects by water quenching

Heating temperature (°C)	Effects on surface morphology	
	Uncoated insert (heated for 30 min and quenched)	Coated inserts (heated for 90 min and quenched)
Up to 700 °C	For uncoated inserts, thermal shock from 900 °C results in significantly different damage mechanisms. a crack network outlined by adjacent homogeneous cells delineates the uncoated outer surface. When WC was shocked at temperatures greater than 800 °C, it exhibited higher retained strengths because of its higher $(K_{1c}/\sigma)_2$ values at these temperatures [20].	The duplex coated (sol-gel TBC) material has a smooth surface with a light texture. In actuality, there are a few tiny cracks beginning to appear around the coated insert's edge (sol gel TBC).
1000–1200 °C	In comparison to coated inserts, uncoated inserts experienced higher deformation and size changes.	Phase diagram changes in the coated insert (sol gel TBC) can be seen. Finally, after 1200 °C then quenching in water freezing, the coated insert (sol-gel TBC) fails due to the propagation of an early fracture, which is likely the beginning of the duplex coating degradation. Can be said that the TiO_2 bond coat interface delamination at the sol-gel TBC deterioration is primarily caused by increasing stress and strain during thermal shock.

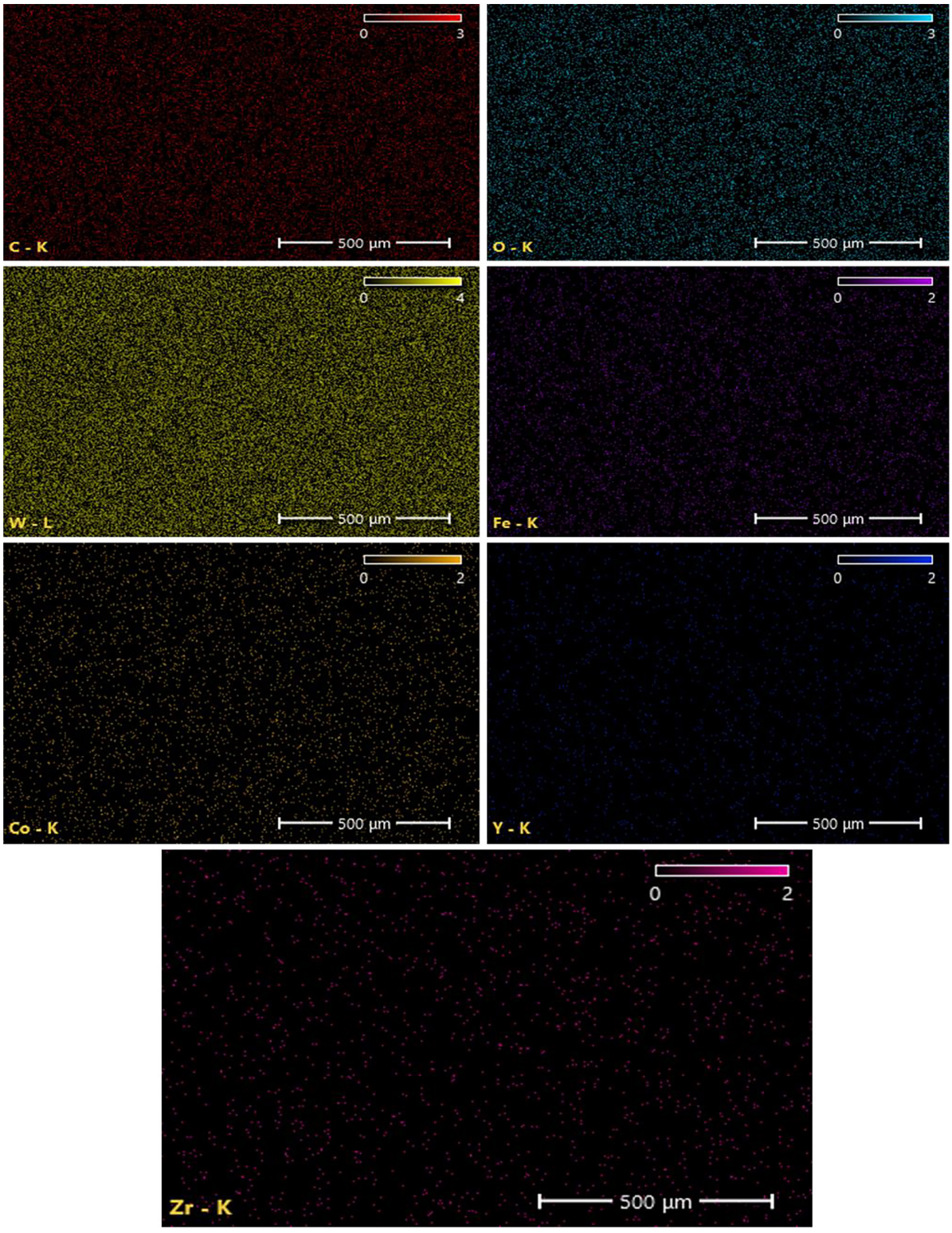

Figure 4. EDS mapping of the prepared duplex layer on the carbide substrate

It is possible to distinguish between coated and uncoated inserts when temperatures rise over 700 to 1200 °C, as illustrated in Table 1 and Figure 6.

During the same sintering for 1200 ℃, at 90 minutes, both samples coated and uncoated fails. In comparison to uncoated inserts, which were subjected to more deformation and changes in dimensions, as shown in Figure 7.

Figure 8 represented the EDS and XRD analysis, can be noticed that heating the uncoated insert at 1200 ℃ for 90 min causes a changes in its phases, mechanical properties, dimensions

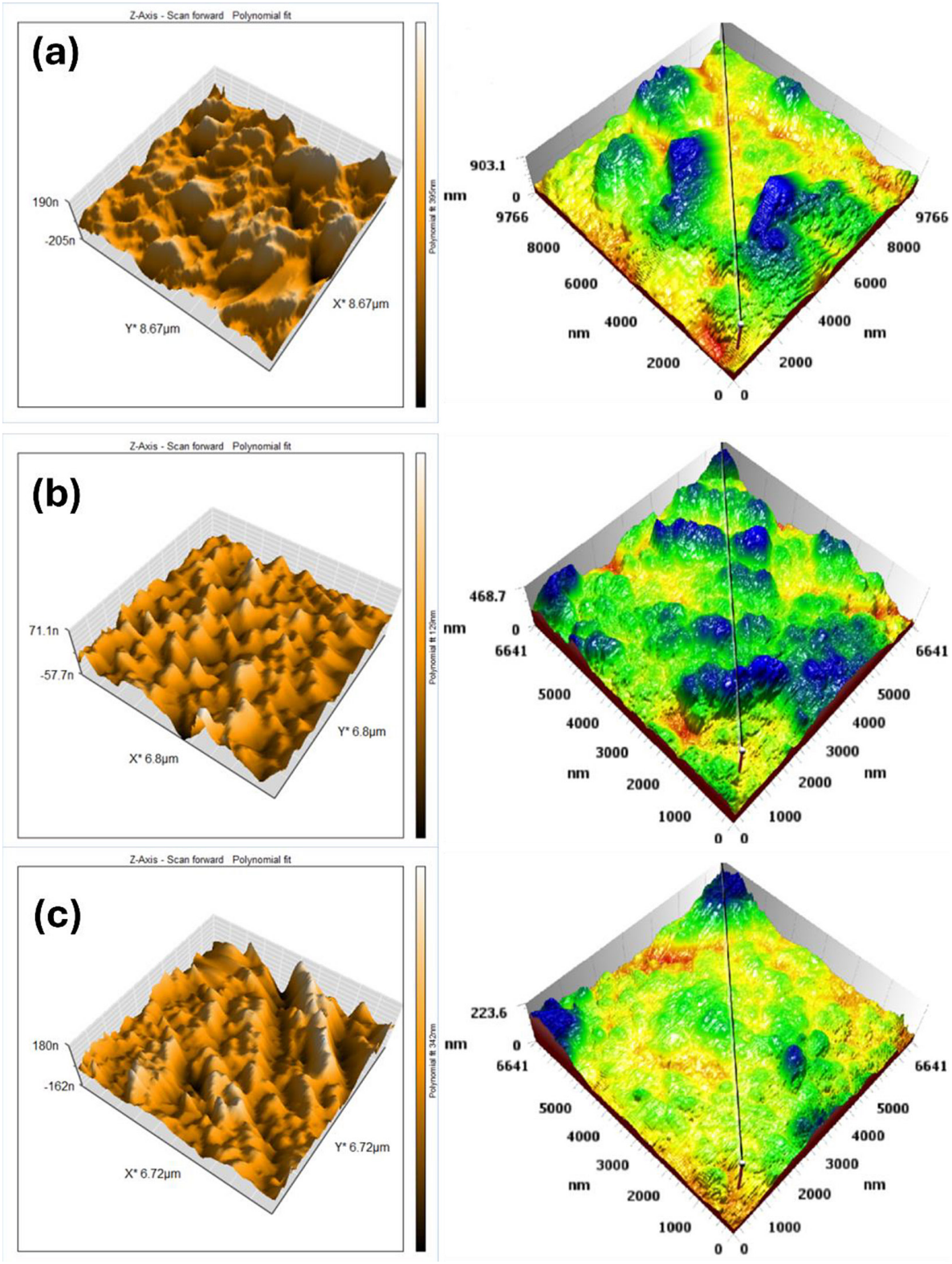

Figure 5. AFM images for a) uncoated insert, b) 8YSZ coating layer, c) TiO_2/8YSZ coating layer

with high deformation, and converts it into brittle structure. Based on XRD analysis of the uncoated insert after the sintering, on amount of TiO_2 was composed.The uncoated insert before sintering has 3.6 wt% CO while percentage reduced to 0.4% due to heating, this caused a reduce in strength and increase the brittleness structure.

In comparison to the diffraction data cards (25–1047), (05–0727) the results for the WC and TiO_2 peaks were shown in Figure 9. The TiO_2

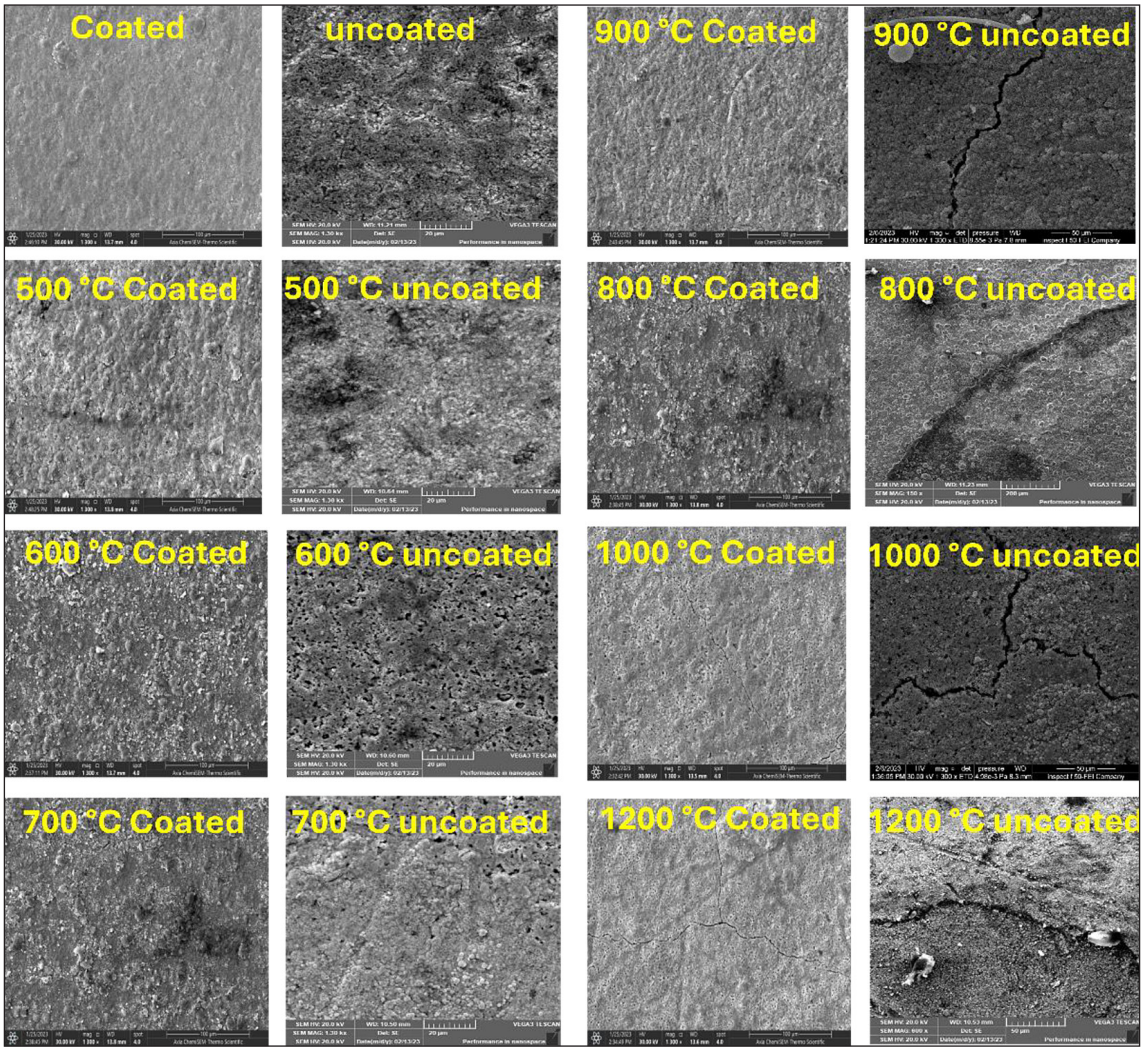

Figure 6. FESEM image of the coated insert sol–gel TBC and uncoated insert after thermal shock process under different conditions

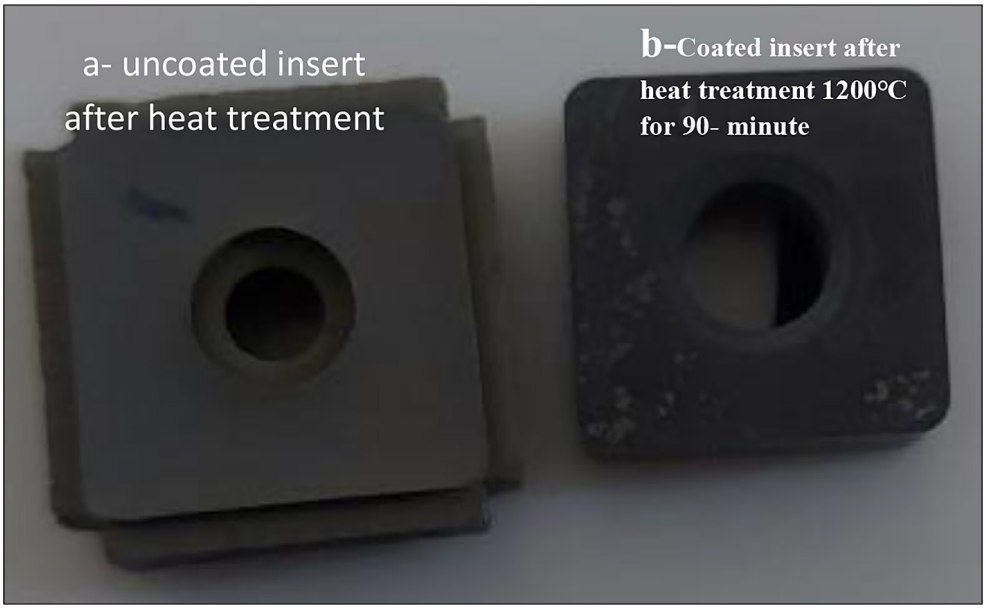

Figure 7. Image after thermal shock at 1200 °C heating for 90 minute then quenching in freezing water about 5 sec a) uncoated insert b) coated insert

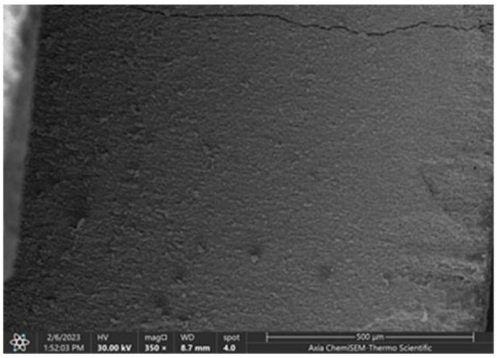

Element	Atomic %	Atomic % Error	Weight %	Weight % Error
C	40.8	1.0	12.6	0.3
O	44.3	1.0	18.2	0.4
Co	0.3	0.1	0.4	0.1
W	14.6	0.2	68.8	1.1
Ti	6.2	0.2	8.1	0.2

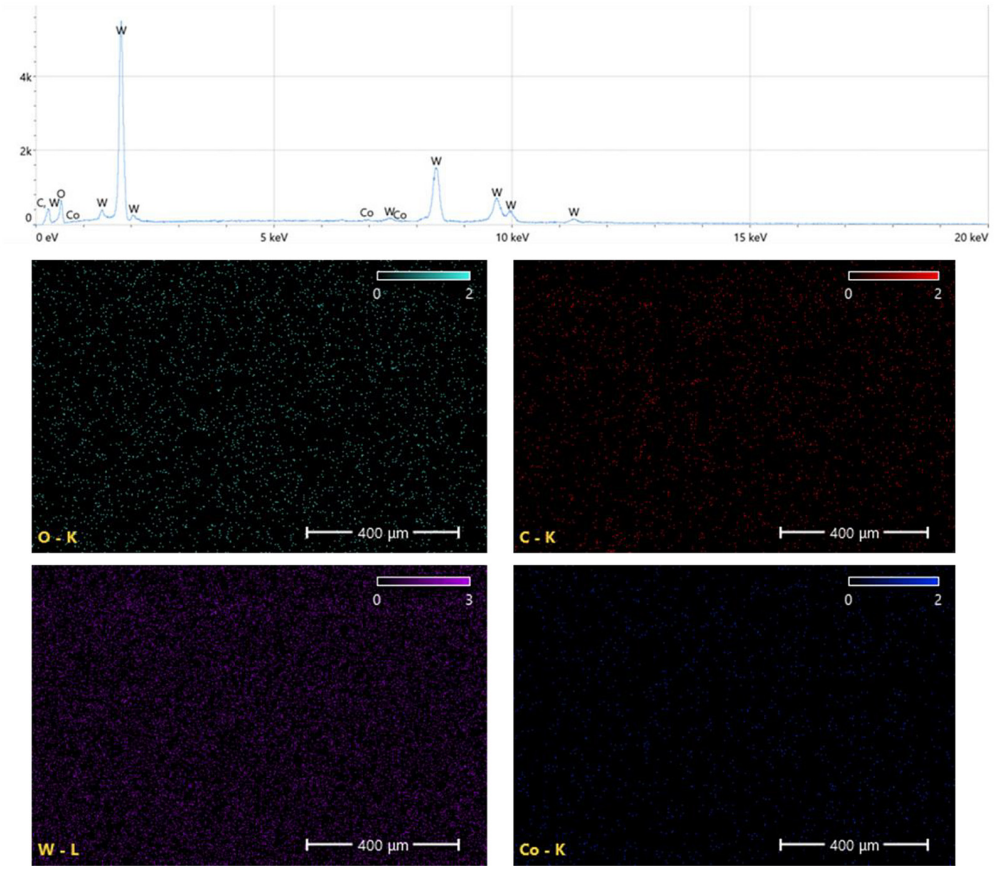

Figure 8. EDS mapping of carbide insert after thermal shock at 1200 °C

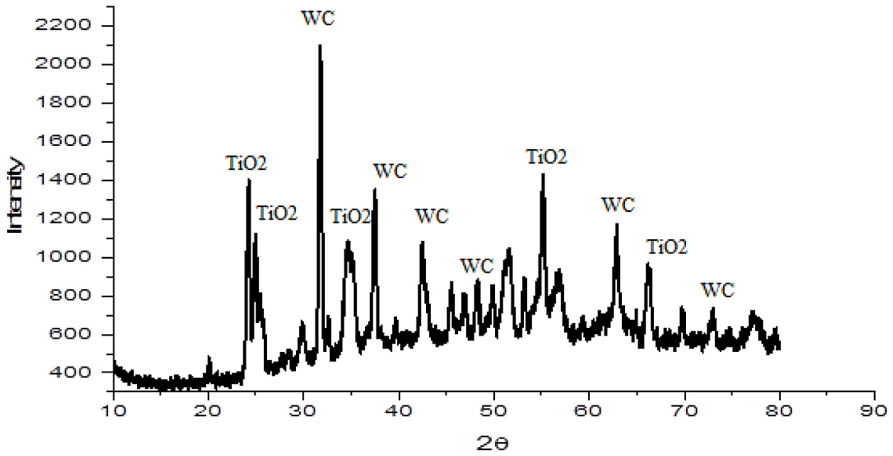

Figure 9. XRD pattern of uncoated insert after thermal shock at 1200 °C

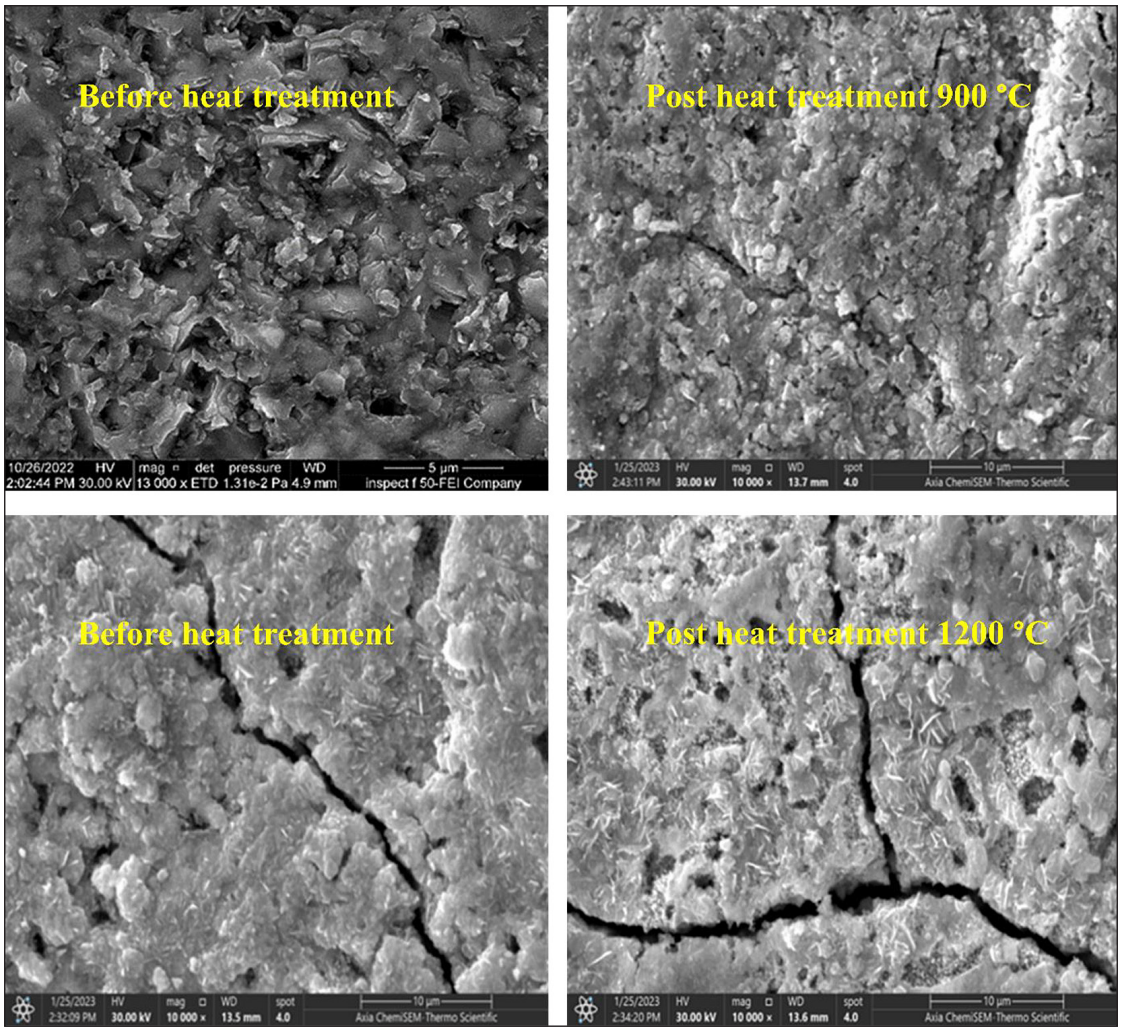

Figure 10. FESEM before and after thermal shock under different conditions for coated inserts

layer after two hours of calcination at 500 °C, which is consistent with the findings of Midab et al. [15]. As may be seen from the multi-phase TiO_2 peaks visible on the diffraction data card (211272). The martensitic phase transformation from the fcc to the hcp phase caused in the cobalt phase after quenching is hypothesized to be connected to the greater strength losses observed for WC-Co hard metals [21].

The macroscopic pictures of the thermal shock-tested nanostructured TBCs. It is evident that failure for every coating began at the sample's edges and spread to the surrounding regions. onset of failure from the edges because of the extreme temperatures experienced there, as well as the singularity of thermal stresses there [22].

In other hand coated insert with TiO_2/8YSZ layers remains as it is for 90 min without any deformation or change in composition although the quenching, spallation due to heating to high temperature 900°C, and then quenching. Phase changes for coated inserts (sol gel TBC) can be seen after thermal shock at 1000 °C, 1200 °C as depicted in Figure 10. Microstructural features like porosity and microcracks have a significant impact on thermal conductivity, which is the primary mechanism for heat transfer at high temperatures [23].

CONCLUSIONS

Based on the results obtained, the following conclusions can be drawn:

- Duplex layer of TiO_2/8YSZ exhibit strong homogeneity, good distribution, and had a minimum average value of surface roughness 223.6 nm comparing 8YSZ layer only.
- The coated insert (duplex coating TiO_2/8YSZ) in this instance really has a few little fractures starting at the edge, after thermal shock from 700 and above (thermal shock), comparing uncoated insert.

- Damage processes for uncoated inserts are dramatically different when subjected to the same conditions of thermal shock.
- After thermal shock at 1000 °C and 1200 °C, coated inserts (sol-gel TBC) can be observed to undergo phase diagram changes.
- During the same thermal shock for 1200 °C, at 90 min, both sample coated and uncoated fails. In comparison to uncoated inserts, which were subjected to more deformation and changes in dimensions.

REFERENCES

1. Al-Ethari H., Al-Dulaimi K.Y., Warcholinski B., Kuznetsova T.A. Interrelation of surface temperature and tribological characteristics of a protective coating on a tool. Journal of Friction and Wear, 2019; 40(6): 603–608.
2. Asaad M, Al-Ethari H., Kareem S.J. Surface modification of cutting tool by multilayer coatings a-Review paper. In: AIP Conference Proceedings 2022; 2660(1): 020093.
3. Cao X., Vassen R., Stoever D. Ceramic materials for thermal barrier coatings. Journal of the European Ceramic Society, 2004; 24(1): 1–10.
4. Bennett A. Properties of thermal barrier coatings. The Institute of Metals. The ceramics processing research and development department of Rolls-Royce Ltd, Derby 1981.
5. Ronghua W., John J.V., Jesse N.M., Michael N.G. Aspects of plasma-enhanced magnetron-sputtered deposition of hard coatings on cutting tools. Surf. Coat. Technol. 2002; 158–159: 465–472.
6. Zhao J. and Liu Z. Influences of coating thickness on cutting temperature for dry hard turning Inconel 718 with PVD TiAlN coated carbide tools in initial tool wear stage, Journal of Manufacturing Processes 2020.
7. Pin L., Vidal V., Blas F., Ansart F., Duluard S., Bonino J.P., Le Maoult Y., Lours P. Optimized sol–gel thermal barrier coatings for long-term cyclic oxidation life. Journal of the European Ceramic Society 2014; 34(4): 961–974.
8. Haenni W., Hintermann H., Morel D., Simmen A. Titania-coatings on strongly passivated substrates.
9. Hajizadeh-Oghaz M., Razavi R.S., Ghasemi A. Synthesis and characterization of ceria–yttria co-stabilized zirconia (CYSZ) nanoparticles by sol–gel process for thermal barrier coatings (TBCs) applications. Journal of Sol-Gel Science and Technology 2015; 74(3): 603–612.
10. Liu L.Y., Shankar R., Howard P. High sintering resistance of a novel thermal barrier coating. Surf Coat Technol 2010; 204(20): 3154–3160.
11. Wang R., Dong X., Wang K., Sun X., Fan Z., Duan W. Two-step approach to improving the quality of laser micro-hole drilling on thermal barrier coated nickel base alloys. Optics and Lasers in Engineering 2019; 121: 406–415.
12. Vignesh B., Oliver W.C., Kumar G.S., Phani P.S. Critical assessment of high speed nanoindentation mapping technique and data deconvolution on thermal barrier coatings. Materials & Design 2019; 181: 108084.
13. Zhao J., Liu Z., Wang B., Hu J., Wan Y. Tool coating effects on cutting temperature during metal cutting processes: Comprehensive review and future research directions. Mechanical Systems and Signal Processing 2021; 150: 107302.
14. ASTM Handbook, Iron and Metal Products 1989; 01.01.
15. Wurood A., Al-Ethari H., Kareem S. Investigation of microstructure, morphology and properties of monolayer and multilayer coating T6-HSS by the sol-gel route, Advances in Materials and Processing Technologies 2022.
16. Yuan K., Yu Y., Wen J.F. A study on the thermal cyclic behavior of thermal barrier coatings with different MCrAlY roughness. Vacuum 2017; 137: 72–80.
17. Pin L., Vidal V., Blas F., Ansart F., Duluard S., Bonino J.P., Le Maoult Y., Lours P. Optimized sol–gel thermal barrier coatings for long-term cyclic oxidation life. Journal of the European Ceramic Society 2014; 34(4): 961–974.
18. Merkleina M., Andreasa K., Engela U. Influence of machining process on residual stresses in the surface of cemented carbides. Procedia Engineering 2011; 19: 252–257.
19. Wurood A.M., Al-Ethari H. and Kareem S.J. 2022. Using grey relation analysis to improve tool life in medium carbon steel turning by coating multilayer HSS insert. In: Proceedings of 13th International Conference on Mechanical and Aerospace Engineering.
20. Mai Y.W. Thermal-shock resistance and fracture-strength behavior of two tool carbides. Journal of the american ceramic society 1976; 59(11–12): 491–494.
21. Tarragó J.M., Dorvlo S., Esteve J., Llanes L. Influence of the microstructure on the thermal shock behavior of cemented carbides. Ceramics International 2016; 42(11): 12701–12708.
22. Luo Q., Jones A.H. High-precision determination of residual stress of polycrystalline coatings using optimised XRD-sin2ψ technique. Surface and Coatings Technology 2010; 205(5): 1403–1408.
23. Pourbafrani M., Razavi R.S., Bakhshi S.R., Loghman-Estarki M.R., Jamali H. Effect of microstructure and phase of nanostructured YSZ thermal barrier coatings on its thermal shock behaviour. Surface Engineering 2015; 31(1): 64–73.